ISSN 1996-3343

Asian Journal of Applied Sciences

http://knowledgiascientific.com

Knowledgia SCIENTIFIC
A Place to Publish Outstanding Research

Asian Journal of Applied Sciences 4 (4): 331-342, 2011
ISSN 1996-3343 / DOI: 10.3923/ajaps.2011.331.342

Supercritical Anti-solvent Process for the Enhancement of Dye-sensitized Solar Cell Efficiency: A Review

[1]S.N.F. Zainudin, [1]M. Markom, [2]H. Abdullah, [3]R. Adami and [1]S.M. Tasirin

[1]Department of Chemical Engineering and Process, Faculty of Engineering and Built Environment, Universiti Kebangsaan Malaysia, 43600 Bangi, Malaysia

[2]Department of Electrical, Electronic and System Engineering, Faculty of Engineering and Built Environment, Universiti Kebangsaan Malaysia, 43600 Bangi, Malaysia

[3]Department of Chemical and Food Engineering, University of Salerno, Via Ponte Don Melillo, I-84084 Fisciano (SA), Italy

Corresponding Author: Siti Nur Fadhilah Zainudin, Department of Chemical Engineering and Process, Faculty of Engineering and Built Environment, Universiti Kebangsaan Malaysia, 43600 Bangi, Malaysia

ABSTRACT

Supercritical Anti-Solvent (SAS) is a promising technique to prepare supported metallic nanoparticles. This review paper highlights the potential of supercritical anti-solvent process in the enhancement of Dye-Sensitized Solar Cell (DSSC) efficiency. The fundamental aspects in SAS process has been applied through the analysis on the controls and modification of main properties of particles such as morphology, size, particle size distribution and crystallinity for the improvement of solar cell application. The current issues and technologies associated with SAS process were stated throughout the study.

Key words: Supercritical anti-solvent, efficiency, solar cell, nanoparticle, photovoltaic performance

INTRODUCTION

The Dye-Sensitized Solar Cell (DSSC) that belongs to the group of thin film solar cells is proposed by O'Regan and Grätzel (1991). It is based on a semiconductor formed between a photo-sensitized anode and an electrolyte, a photoelectrochemical system. Dye Sensitized Solar Cells (DSSC) is one of the efficient and promising alternative clean energy harvesting technology to directly convert solar energy into electricity as it only requires a low production cost and low environmental impact during fabrication. A typical DSSC is composed of a Transparent Conductive Oxide (TCO) glass such as F-doped SnO_2 glass (F/SnO_2) covered with nanocrystalline TiO_2, dye molecules attached to the surface of TiO_2, an electrolyte containing a redox couple (I^-/I_3^-) and a counter electrode such as a Pt deposited TCO glass (Fig. 1). The nano-sized of TiO_2 makes large amount of dye can be adsorped due to the large surface area of nanocrystalline TiO_2. Photoexcitation of the dye injects an electron into the conduction band of TiO_2. The electron can be conducted to the outer circuit to drive the load and making the electric power (Xiaobo, 2009; Gratzel, 2004). Hence, the nanocrystalline TiO_2 structure plays a major role in the enhancement of DSSC efficiency.

Recently, several studies have been utilized to improve the performance of the DSSC. Alonso *et al.* (2007) states that the control of particle size, crystallinity and surface area is very important for solar cell efficiency. They studied the effect of operational parameters on the synthesis

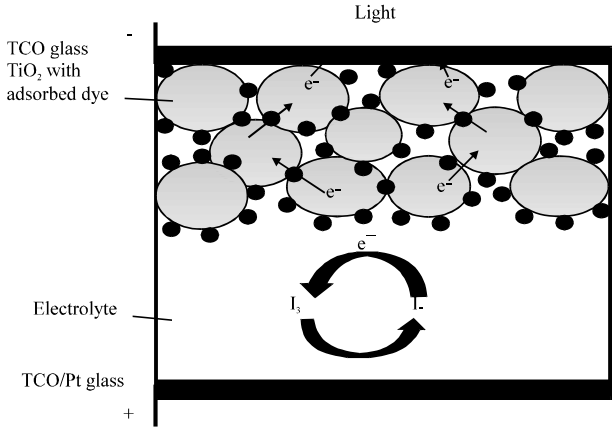

Fig. 1: The structure and mechanisms of dye-sensitized solar cell

of TiO_2 particles such as particle morphology, Particle Size Distribution (PSD), specific surface area and crystallinity by using two different precursors which is diisopropoxititanium bis(acetylacetonate) (DIPBAT) and titanium tetraisopropoxide (TTIP). Shi *et al.* (2009) has studied the effect of TiO_2 layer derived by pretreating the TCO with $TiCl_4$ aqueous solution, on the performance of the DSSC. The TiO_2 compact layer can effectively control the dark current at lower voltages, which is beneficial to enhance the conversion efficiency (η) due to the improvement of open circuit voltage (v_{oc}) and Fill Factor (FF). Tsai and Lu (2009) has obtained a studies of the improvement of the light to electricity conversion efficiency of the DSSC by enhancing the scattering of the incident light within the cell, most often through addition of a light scattering structure on top of the photo-anode layer, to better utilize the light for electron generation.

Some research also has been carried out on the modifications of the film structure as an effort to improve the efficiency in DSSC application. Pollou *et al.* (2009) developed a wave-like microstructure titanium layer which is obtained by electro-polishing processes. The surface texture of the layer typically contains sharp corners and depends strongly upon the underlying crystallite orientation and morphology. Its benefit is most significant in the designs that use a very thin photoactive layer with high quantum efficiency, which is light that is not utilized in the energy conversion process, is refiected rather than absorbed. Paulose *et al.* (2006) developed nanotube array electrodes in DSSC system to reduce losses incurred by charge-hopping across nanoparticle grain boundaries. The ordered nanostructured allows larger electron lifetimes and a suppression of back electron transfer from electrode to electrolyte. The nanotube layer has been further improved by Wang *et al.* (2010) whom developed a DNA-like structured DSSC which offers a high surface area for the absorption of sunlight from any directions. However, for this type of structure, it is necessary to use other colourless redox couple system instead of the traditional high absorbance iodine-based electrolyte as the sunlight has to pass through the electrolyte first and then gets to the surface of anode.

Kawasaki *et al.* (2009) states that at industrial stage, it is necessary to produce nanoparticles of smaller size with a narrow size distribution, controllable size and high crystallinity at low manufacturing costs using a green process route. The effectiveness of titania as a photocatalyst depends on its crystal phase, particle size and crystallinity which are greatly influenced by the

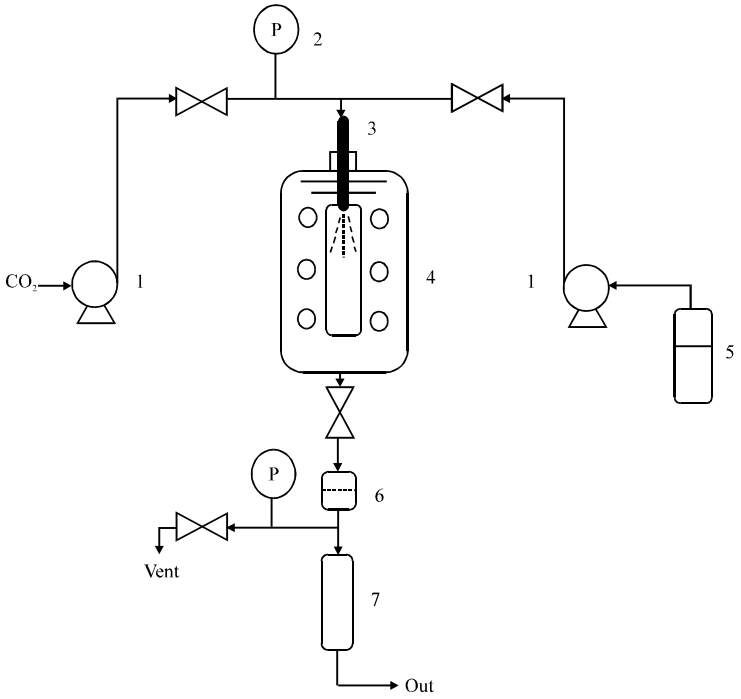

Fig. 2: Schematic diagram of Supercritical Anti-Solvent apparatus (1: High pressure pump; 2: Pressure gauge; 3: Injector nozzle; 4: Jurguson vessel; 5: Solution mixture; 6: Filter; 7: Phase separator)

preparation methods (Binitha *et al*., 2009). Recently, the research on supercritical technology has become a major interest and has been widely applied, mostly in pharmaceutical and biological additives application. The use of supercritical fluids process make it possible to obtain a dry and clean product, with a simpler one-step process, avoiding subsequent purification stages and minimizing particle agglomeration, in comparison with the conventional methods of micronization (Sierra-Pallares *et al*., 2009). However, the study that relates supercritical antisolvent process with the efficiency of solar cell application is still lacking. The supercritical antisolvent process as shown schematically in Fig. 2, offer a great benefits in the simple modification and controlling of particle formation to achieve the desired characteristics. The SAS process is usually operated as follows: a supercritical-CO_2 is delivering to the precipitation chamber until the desired pressure is reached. When antisolvent steady flow is established, pure solvent is sent through the nozzle to the chamber. When a quasi-steady state composition of solvent and antisolvent is realized within the precipitator, the flow of the pure solvent is stopped and the liquid solution is delivered through the nozzle, producing the precipitation of the solute. At the end of the liquid solution delivery, the chamber is purged with supercritical CO_2 to wash it from the residual solvent solubilized in the supercritical antisolvent. SAS processing also benefits from the rapid mass transfer occurring in supercritical fluids due to their lower viscosity and higher diffusivity relative to liquids (Gokhale *et al*., 2007). Thus, in this paper, we highlight the findings on the potential of SAS process in the improvement of solar cell efficiency by controlling the properties of TiO_2 nanoparticles.

CONTROL OF NUCLEATION AND CRYSTAL GROWTH KINETICS

The nucleation and particle growth affects the final size of the particles and particle size distribution. The particle formation is controlled by phase equilibrium, mass transfer and chemical reaction. Dukhin *et al.* (2005) states that major sub-processes of the solute nucleation involve droplet formation, droplet interaction and coagulation together with droplet mass transfer. The droplet residence time, τ_{res} and precipitation time that affects the nanoparticle dimension is controlled by the stream velocity which led to the rate of turbulent droplet coagulation.

Alonso *et al.* (2007) states that the nucleation process in supercritical fluid can be described by the growth of particles through condensation and coagulation. The solubility of desired solid product initiates the nucleation step and the precipitation of the product controlled by the supersaturation degree of the medium. Hence, the size of the particles is inversely proportional to the supersaturation degree of the medium. The mixture formation between the solvent and the antisolvent is the vital issue in producing fine and uniform particle (Cansell and Aymonier, 2009; Aymonier *et al.*, 2006; Dowy *et al.*, 2009a, b). Dowy *et al.* (2009a, b) studied a homogenous mixture on the molecular scale, prior to nucleation and particle growth, as the homogenous solute supersaturation will lead to a uniform particle size distribution. In the experiment, the injected liquid experiences the progressive disappearance of the interfacial tension and the droplets are not formed as the interfacial tension reduces to zero before jet break-up for both solvents. At single-phase mixing conditions, solidification of the solute has to be attributed to the classical gas-to-particle nucleation and the subsequent growth mechanism. Gas-to-solid particle formation is characterized by nucleation, followed by a reduced growth since mass transfer from the bulk of the gas phase to the surface of the particle is poor, as the solute is practically not soluble in the fluid phase.

The jet fluid dynamics has a vital effect on reaction rate as it controls the mass transfer and phase equilibrium process in supercritical phase. Reverchon *et al.* (2009a, b) studied the jet fluid dynamics using thin wall injectors for the investigation of the liquid solvents acetone and DMSO at operating conditions of 40°C in the pressure range between 6 and 16 MPa, where the break-up length of the jet is studied and correlated as a function of the Reynolds and Ohnesorge numbers. When SAS is performed at supercritical conditions, a transition between multi-phase and single-phase mixing is observed by increasing the operating pressure. Single-phase mixing is due to the very fast disappearance of the interfacial tension between the liquid solvent and the fluid phase in the precipitator. The transition between these two phenomena depends not only on the operating pressure, but also on the viscosity and the surface tension of the solvent. Indeed, single-phase mixing has been observed for acetone very near the mixture critical point, whereas DMSO showed a progressive transition for pressures of about 12 MPa. Later, Reverchon *et al.* (2009a, b) study the interaction of emulsion droplets with the atomization process. Indeed, SAS atomization at subcritical and near critical conditions produces organic solvent droplets that can contain one or more micelles. During the atomization, micelles can be disturbed by the shear stress due to the jet break-up and the final result could be a partial disaggregation or reorganization of the micelles that can produce smaller particles. In a well-developed supercritical condition (150 bar, 35°C), no droplets exists and the process evolves as a single phase mixing. If droplets of the less soluble aqueous solution are contained in the liquid phase, they can be subject to a stronger perturbation (since the external liquid shell of the continuous phase is not formed as in the SAS at subcritical and near critical conditions).

Dowy *et al.* (2009a,b) studied the rapid mixture formation during high-pressure injection of liquid ethanol into supercritical CO_2 to investigate the density distribution during the injection process. From the research, they found no influence of the injected ethanol on the density distribution of CO_2 in the condition above the Mixture Critical Point (MCP). During the penetration of the injected ethanol into the CO_2, the surface tension vanishes, driven by the mixing process and a homogeneous supercritical mixture is generated. As no droplets are formed because of the none existence of interface tension, neither absorption of CO_2 nor evaporation of the droplets occurs. Later Dowy *et al.* (2009a, b) carried out an investigation on the influence of solute onto the phase behavior of the pseudo-binary system ethanol/ CO_2 in the supercritical antisolvent process. The studies highlight the influence of the solute on the mixing mechanisms between the injected solution and the antisolvent from homogeneous supercritical jet mixing to multi-phase mixing with particle precipitation from liquid phase. At conditions above the MCP, the mixing process is gas-like and therefore characterized by turbulent flow and vortices in the jet structure. The variation in process conditions from below the MCP to above the MCP of the binary mixture ethanol/ CO_2 and the variation of the temperature clearly stated that mixture formation can be influenced between spray and jet mixing mechanisms by changing the CO_2 pressure and therefore with the density of the antisolvent. Changing the injection pressure result in comparatively small variations in the mole fraction distribution but cannot influence the phase behavior of the mixing mechanism. Precipitation from a fully developed supercritical single-phase maybe possible at higher pressures, where the CO_2 partial density within the mixing regime and the bulk density of CO_2 within the SAS chamber converge.

Very few works has been performed towards the development of numerical models to predict the growth of nanoparticles. Mostafa Nowee *et al.* (2008) developed a model based on a population balance approaches to describe the dynamic change of particle size in crystallization processes under the effect of antisolvent addition in identifying the nucleation and growth kinetic in the crystallization of particle. They found that the feed rate at the early stages of the process is crucial as it defines the outcomes of the final particle size characteristics due to the formation of a high peak of supersaturation at the early stages of the process when primary nucleation occurs. Sierra-Pallares *et al.* (2009) developed a comprehensive mathematical model to estimate the average diameter attained by the particles that are being generated by supercritical fluid process. The model is solved by using CFD (Computational Fluid Dynamics) for the experimental geometry consists of a tee piece as mixed and cylindrical reactor. The model was applied to the system of CO_2-ethanol-DIPBAT (diisopropoxititanium bis(acetilacetonate)). The monodisperse model has been used to describe integral properties of particle size distribution such as concentration, aerosol volume and particle diameter. The results of this investigation allowed to a conclusion that the residence times and the Reynolds numbers have a strong influence on the control of particle formation. Erriguible *et al.* (2009) also developed a monodisperse model of particle growth in supercritical fluid process based on two steps mechanism which is coalescence followed by aggregation mechanism, to predict the evolution of primary particle size and the number of primary particles per aggregate to estimate the aggregate size in the reactor as a function of the operating parameters which is pressure, temperature, precursor concentration and residence time. The population balance equation is solved by assuming a monodisperse distribution. This model describes the evolution of particles by the variation of the particle concentration, the volume and the average surface of aggregates.

CONTROL OF SIZE AND PARTICLE SIZE DISTRIBUTION

Nanostructured materials have offered new opportunities in designing a more efficient solar cells, by facilitating photon absorption, electron transport and electron collection. Nanostructures are promising for photovoltaic devices due to several performance and processing benefits, such as a direct path for charge transport and large surface areas for light harvest offered by the geometry of such nanostructures (Yu and Chen, 2009). The nanosize particles provide a wide band gap which allows electron injection from the excited state of the dye in DSSC application. A large surface area of nanoparticles gives an efficient interfacial transfer and allows absorption of large amount of dye. When size of the particle decreased, the fraction of atom located on the surface increased with higher surface area to volume ratios which led to the enhancement of photocatalytic activity (Xiaobo, 2009). The reduction of particle size also led to an increased of the photoredox reactions due to the increased of redox potential of the valence-band holes and the conduction band electrons.

Many research evaluate that the growth of particles is directly related to mass transfer (Alonso *et al*., 2007; Erkey, 2009; Argemi *et al*., 2009; Park and Yeo, 2008a, b; Shariati and Peters, 2003). The collission between the nuclei or new material adhesion to form the particles are controlled by mass transfer (Alonso *et al*., 2007). The mixing of reactants and diffusion are favored by turbulence. Sierra-Pallares *et al*. (2009) proposed a pseudo-first order kinetic for the extinction of the chemical precursors. In the studies of the preparation of nanoparticles by supercritical fluid processes, Reverchon and Adami (2006) stated that in the supercritical antisolvent precipitation process, the supercritical fluid should be completely miscible with the liquid solvent; whereas, the solute should be insoluble in the supercritical fluid (SCF). Therefore, contacting the liquid solution with the SCF induces the formation of a solution, producing supersaturation and precipitation of the solute. The formation of the liquid mixture is very fast due to the enhanced mass transfer rates that characterize supercritical fluids and as a result, nanoparticles could be produced. An important role in enhancing the mass transfer is also played by the liquid solution injection device. The injector is designed to produce liquid jet break-up and the formation of small droplets to produce a large mass transfer surface between the liquid and the gaseous phase.

Petit-Gas *et al*. (2009) studied the jet dispersion of liquid organic solvents in supercritical continuous phase under miscible conditions but just above the mixture critical point. This study highlights the influence of hydrodynamics upon the powder characteristics for generated particles using SAS process. The result from their experiments shows that the key-point to form finer particles appears to be the mixing state more than the atomization state even if the characteristics powder are more homogeneous when the jet is atomized. For the same velocity jet, finer particles are formed for higher jet Reynolds numbers. Based on their studies, it is essential to also consider and characterize the hydrodynamic jet conditions in the vessel for the interpretation of crystallization of particles in SAS process. In conjunction with hydrodynamic properties (Barrett *et al*., 2008) reported that the decreased of particle size can be attributed to the higher carbon dioxide density which increases the deforming pressure forces necessary to break up the liquid droplet into smaller droplets hence creating smaller particles. As a summary, as shown in Table 1, the size of particles can be varied by the controlling of mass transfer and jet dynamics by the variation of process parameters.

Table 1: Different morphologies and sizes of the particles derived by SAS process

		Condition parameters							
				Conc.	Solvent flowrates	CO_2 flowrates			
Compound	Solvent	T (°C)	P (bar)	wt (%)	---------(mL min^{-1})----------		Shape	Size	Ref.
TiO_2	Ethanol	300	200	21	2	8.3	Spherical	25-400	Hakuta *et al.* (2003)
TiO_2	Ethanol	300	200	21	2.4	9.7	Spherical	22-350	Hakuta *et al.* (2003)
TiO_2	Ethanol	300	200	21	3.6	14.5	Spherical	14-300	Hakuta *et al.* (2003)
TiO_2	Ethanol	300	200	21	7.2	29	Spherical	11-250	Hakuta *et al.* (2003)
TiO_2	Ethanol	300	200	21	11	44	Spherical	14-220	Hakuta *et al.* (2003)
WO_3	i-octane	35	100	40	2		Spherical	60-80	Reverchon *et al.* (2009a, b)
WO_3	Cyclohexane	35	150	40	2		Spherical	24-34	Reverchon *et al.* (2009a, b)
WO_3	Ethyl Acetate	35	150	40	2		Spherical	10	Reverchon *et al.* (2009a, b)
WO_3	Cyclohexane	36	70	40	2		Spherical	500	Reverchon *et al.* (2009a, b)
SiO_2	Cyclohexane	35	100	40	2		Spherical	500	Reverchon *et al.* (2009a, b)
MoO_3	Cyclohexane	35	150	40	2		Spherical	10-100	Reverchon *et al.* (2009a, b)
Yac	DMSO	40	150	5*	2		Spherical	20-100	Reverchon *et al.* (2007)
Gdac	DMSO	40	150	100*	2		Spherical	100-500	Reverchon *et al.* (2007)
Amoxicilin	NMP	40	150	20*	2		Spherical	100-500	Reverchon *et al.* (2007)
Rifampicin	DMSO	40	150	10*	2		Spherical	70-100	Reverchon *et al.* (2007)
Astemizole	DMSO	40	150	10*	2		Spherical	100-300	Reverchon *et al.* (2007)
HMX	DMSO	40	150	5	2	15	Needles	13.4*	Kim *et al.* (2009)
HMX	DMF	40	151	2	2	15	Plates	7.8*	Kim *et al.* (2009)
HMX	Cyclohexane	40	152	2	2	15	Prisms	6.1*	Kim *et al.* (2009)
HMX	Acetone	40	153	2	2	15	Prisms	9.5*	Kim *et al.* (2009)
HMX	NMP	40	154	2	2	15	Plates	4.1*	Kim *et al.* (2009)
Phenylbutazone	Acetone	35	95	30		0.61*	Needles	6.8-56.5*	Park and Yeo (2008a, b)
Phenylbutazone	Acetone	35	95	30		16.70*	Needles	3.2-15.5*	Park and Yeo (2008)
CeO	Methanol	40	110	13.33*	0.1	7	Spherical	3-8 nm	Tang *et al.* (2007)
CeO	Methanol	40	150	13.33*	0.1	7	Spherical	3-8 nm	Tang *et al.* (2007)
CeO	Methanol	60	110	13.33*	0.1	7	Spherical	3-8 nm	Tang *et al.* (2007)

*Concentration of precursor in mg mL^{-1}, CO_2 flowrates in bar/min and size in μm range

CONTROL OF PARTICLE MORPHOLOGIES

Morphologies attract significant interest due to their potential applications in microelectronics, interconnections, optoelectronics and as nanoscale electronic devices (Aymonier *et al.*, 2006). Zhao *et al.* (2010) found that the morphology of the particles produced is depends on the position of operating point with respect to the mixture critical point of ternary systems. By varying the critical pressure and temperature, different morphologies were obtained. From the studies, the presence of spherical microparticles were obtained in a completely developed supercritical phase region, while an irregular sphere and a plate-like microparticle were obtained in an operating condition near supercritical region and in a subcritical condition, respectively. Reverchon *et al.* (2008) states that the spherical particles are the result of droplets drying after effective atomization of the liquid solution. At pressure far above the critical pressure, the spherical nanoparticles are consistently produced by precipitation from the fluid phase. Reverchon *et al.* (2007) studied the morphology of the microparticles formed during SAS precipitation at the different process conditions and found a correlation between particle morphology and the observed jet fluid dynamics. Expanded microparticles were obtained working at subcritical conditions; whereas spherical microparticles were obtained operating at supercritical conditions up to the pressure where the transition between multi-phase and single-phase mixing was observed. Nanoparticles were

obtained at far above the mixture critical pressure. During this condition, the fluid dynamic behavior acts as a single phase mixing. Park and Yeo (2008a, b) found that the crystal obtain in SAS process have better external shape compare from conventional method which is solvent evaporation method. In their studies, they obtain a regular external shape with a clean surface texture and sharp angles for the particles produced by SAS process compare to the particles produced by solvent evaporation process which have a significant agglomeration problem. In summary, data in Table 1 presents a wide range of particle morphologies produced by SAS process by the variation of parameters condition.

CONTROL OF CRYSTALLINITY AND SPECIFIC SURFACE AREA

Kawasaki *et al.* (2009) have developed a fast micromixing method using high temperature by applying supercritical CO_2 synthesis. Based on their study, the crystallinity of the particles can be improved by increasing the residence time in a constant high temperature. A large surface area may lead to an increase of photocatalytic activity; however, it also becomes a defective site led to a faster recombination. Therefore, the improvement of the crystallinity of particles can reduce the bulk defects and enhance the photocatalytic activity (Xiaobo, 2009). High temperature treatment usually improves the crystallinity of TiO_2 nanomaterials, which in return can induce the aggregation of small nanoparticles and decrease of the surface area (Xiaobo, 2009; Alonso *et al.*, 2007). However, increment of temperature treatment can reduce the fill factor of the cell due to the degradation of conductive layer by oxidation (Ngamsinlapasathian *et al.*, 2006). Park and Yeo (2008a, b) has studied the effect of SAS on the degree of crystallinity. They observed that the degree of preferred orientation could be controlled by varying the CO_2 injection rate. From their studies, the slow injection rate of CO_2 may facilitate the molecules to arrange in a particular orientation during the packing inside the crystalline lattice.

However, some study found that for non-doped TiO_2, less than 5% of solar energy are absorbed; therefore, numerous studies have been conducted to enhance the interfacial charge-transfer reaction and narrows the band gap of TiO_2 which led to the increasing of photo-reactivity of TiO_2 (Chen *et al.*, 2009) such as doping of TiO_2 by carbon (Chu *et al.*, 2008), nitrogen (Dong *et al.*, 2009; Joshi *et al.*, 2009), phosphorous (Jin *et al.*, 2009) and rare earth elements (Stengl *et al.*, 2009). Doping of the film can improve the crystallinity (Pu *et al.*, 2010) and specific surface area (Tian *et al.*, 2009) of the prepared solar cell to increase their conductivities (Liu *et al.*, 2010) by shifting the optical absorption edge of TiO_2 toward lower energy region, thereby increasing the photosensitivity of material (Xiaobo, 2009; Ao *et al.*, 2009; Chu *et al.*, 2008). Current doping process on TiO_2 involves a high temperature treatment and a long time of hydrothermal treatment (Jin *et al.*, 2009; Pu *et al.*, 2010), both of which are unfavorable in energy as high temperature can degrade the conductive layer of the cell by oxidation (Chen *et al.*, 2008). Therefore, SAS is chosen as it offers a mild condition process and a rapid recrystallization process. SAS process also offers a more flexibility in designing the characteristics of a given materials which results in higher yields and provide a wide range of possibilities for in-situ doping (Aymonier *et al.*, 2006).

SAS DESIGN CONFIGURATION AND SCALE-UP IMPLEMENTATION

Calvignac and Boutin (2009) have introduced a new mixing contacting device based on the impinging jets technology to help the micronized molecules dissolved in an appropriate organic solvent. The technique consists of arranging two jets in face to face position in order to generate a zone of high turbulence and favor the mass transfer. The study highlight the influence of operating

parameters and geometric parameters of the impinging jets device which is the jet velocity, impinging distance, organic solvent and solute concentration on particle size and particle size distribution. They found that compared to traditional SAS process, the impinging jet device allows a significant reduction on particle size from few millimeters to 10 μm.

Jarmer *et al.* (2006) studied the different criteria for scaling up the nozzle in the precipitator. They observed that the best scale-up criterion was a constant energy dissipation rate in the nozzle, while maintaining a constant Reynolds number. Adami *et al.* (2008) found that the efficiency of the atomization device and the droplets distribution in the spray influence the diameter of the products produced. They obtained the same morphology of particles when similar operating conditions of the key process parameters were used in their scaling-up comparison studies.

CONCLUSION

The analysis of literature results has confirmed that the SAS technology is a reliable process which allows the production of well designed materials with controlled properties and can be consistently used to manufacture spherical nanoparticles with a high crystallinity and low particle size distribution which are the major characteristics of the particles used for the improvement of dye-sensitized solar cell efficiency. By focusing on the modification of particle which is the main structure of the film in solar cell applications, SAS technology allows the control of morphology, crystallinity and particle size distribution of the particles. The fundamental mechanisms of SAS precipitation process such as high pressure phase equilibria, fluid dynamics and mass transfer are fundamentally essential in the modification and controls of particle characteristics. Many efforts have been carried out through the research development of theoretical models and experiments. These attempts are indeed necessary for development of systematic procedures for the design and scale-up for commercial application of SAS process in solar cell industry.

REFERENCES

Adami, R., E. Reverchon, E. Jarvenpaa and R. Huopalahti, 2008. Supercritical antisolvemt micronization of nalmefene HCl on laboratory and pilot scale. Powder Technol., 182: 105-112.

Alonso, E., I. Montequi, S. Lucas and M.J. Cocero, 2007. Synthesis of titanium oxide particles in supercritical CO_2: Effect of operational variables in the characteristics of the final product. J. Supercritical Fluids., 39: 453-461.

Ao, Y., J. Xu, D. Fu and C. Yuan, 2009. A simple method to prepare N-doped titania hollow spheres with high photocatalytic activity under visible light. J. Hazardous Mater., 167: 413-417.

Argemi, A., A. Vega, P. Subra-Paternault and J. Saurina, 2009. Characterization of azacytidine/poly(L-lactic) acid particles prepared by supercritical antisolvent precipitation. J. Pharmac. Biomed. Anal. 50: 847-852.

Aymonier, C., A. Loppinet-Serani, H. Reveron, Y. Garrabos and F. Cansell, 2006. Review of supercritical fluids in inorganic material science. J. Supercritical Fluids, 38: 242-251.

Barrett, A.M., F. Dehghani and N.R. Foster, 2008. Increasing the dissolution rate of itraconazole processed by gas antisolvent techniques using polyethylene glycol as a carrier. Pharmaceut. Res., 25: 1274-1289.

Binitha, N.N., Z. Yaakob, M.R. Reshmi, S. Sugunan, V.K. Ambili and A.A. Zetty, 2009. Preparation and characterization of nano silver-doped mesoporous titania photocatalysts for dye degradation. Catalysis Today, 147: 76-80.

Calvignac, B. and O. Boutin, 2009. The impinging jets technology: A contacting device using a SAS process type. Powder Technol., 191: 200-205.

Cansell, F. and C. Aymonier, 2009. Review of Design of functional nanostructured materials using supercritical fluids. J. Supercritical Fluids, 47: 508-516.

Chen, F., W. Zou, W. Qu and J. Zhang, 2009. Photocatalytic performance of a visible light TiO_2 photocatalyst prepared by a surface chemical modification process. Catalysis Communic., 10: 1510-1513.

Chen, J., M. Yao and X. Wang, 2008. Investigation of transition metal ion doping behaviours on TiO_2 nanoparticles. J. Nanoparticles Res., 10: 163-171.

Chu, D., X. Yuan, G. Qin, M. Xu, P. Zheng, J. Lu and L. Za, 2008. Efficient carbon-doped nanostructured TiO_2 (anatase) film for photoelectrochemical solar cells. J. Nanoparticles Res., 10: 357-363.

Dong, L., Y. Ma, Y. Tian, G. Ye, X. Jia and G. Cao, 2009. Preparation and characterization of nitrogen-doped titania nanotubes. Mater. Lett., 63: 1598-1600.

Dowy, S., A. Braeuer, K. Reinhold-Lopez and A. Leipertz, 2009a. Laser analysis of mixture formation and the influence of solute on particle precipitation in the SAS process. J. Supercritical Fluids, 50: 265-275.

Dowy, S., A. Braeuer, R. Schatz, E. Schluecker and A. Leipertz, 2009b. CO_2 partial density distribution during high-pressure mixing with ethanol in the supercritical antisovent process. J. Supercritical Fluids, 48: 195-202.

Dukhin, S.S., Y. Shen, R. Dave and P. Pfeffer, 2005. Droplet mass transfer, intradroplet nucleation and submicron particle production in two-phase flow of solvent-supercritical antisolvent emulsion. Colloids Surfaces Physicochem. Eng. Aspects, 261: 163-176.

Erkey, C., 2009. Preparation of metallic supported nanoparticles and films using supercritical fluid deposition. J. Supercritical Fluids, 47: 517-522.

Erriguible, A., F. Marias, F. Cansell and C. Aymonier, 2009. Monodisperse model to predict the growth of inorganic nanostructured particles in supercritical fluids through a coalescence and aggregation mechanism. J. Supercritical Fluids, 48: 79-84.

Gokhale, A., B. Khusid, R.N. Dave and R. Pfeffer, 2007. Effect of solvent strength and operating pressure on the formation of submicrometer polymer particles in supercritical microjets. J. Supercritical Fluids, 43: 341-356.

Gratzel, M., 2004. Review of dye-sensitized solar cells. J. Photochem. Photobiol. C. Photochemis. Rev., 4: 145-153.

Hakuta, Y., H. Hayashi and K. Arai, 2003. Fine particle formation using supercritical fluids. Current Opinion Solid State Mater. Sci., 7: 341-351.

Jarmer, D.J., C.S. Lengsfeld and T.W. Randolph, 2006. Scale-up criteria for an injector with a confined mixing chamber during precipitation with a compressed-fluid antisolvent. J. Supercritical Fluids, 37: 242-253.

Jin, C., R.Y. Zheng, Y. Guo, J.L. Xie, Y.X. Zhu and Y.C. Xie, 2009. Hydrothermal synthesis and characterization of phosphorous-doped TiO_2 with high photocatalytic activity for methylene blue degradation. J. Mol. Catalysis Chem., 313: 44-48.

Joshi, M.M., N.K. Labhsetwar, P.A. Mangrulkar, S.N. Tijare, S.P. Kamble and S.S. Rayalu, 2009. Visible light induced photoreduction of methyl orange by N-doped mesoporous titania. Applied Catalysis Gen., 357: 26-33.

Kawasaki, S.I., Y. Xiuyi, K. Sue, Y. Hakuta, A. Suzuki and K. Arai, 2009. Continuous supercritical hydrothermal synthesis of controlled size and highly crystalline anatase TiO_2 nanoparticles. J. Supercritical Fluids, 50: 276-282.

Kim, C., B. Lee, Y. Lee and H.S. Kim, 2009. Solvent effect on particle morphology in crystallization of HMX (cyclotetramethylenetetranitramine) using supercritical carbon dioxide as antisolvent. Korean J. Chem. Engin., 26: 1125-1129.

Liu, Z., C. Liu, J. Ya and E. Lei, 2010. Preparation of ZnO nanoparticles and characteristics of dye-sensitized solar cells based on nanoparticles film. Solid State Sci., 12: 111-114.

Mostafa Nowee, S., A. Abbas and J.A. Romagnoli, 2008. Antisolvent crystallization: Model identification, experimental validation and dynamic simulation. Chem. Engin. Sci., 63: 5457-5467.

Ngamsinlapasathian, S., S. Pavasupree, S. Y. Suzuki and S. Yoshikawa, 2006. Dye-sensitized solar cell made of mesoporous titania by surfactant-assisted templating method. Solar Energy Mater. Solar Cells, 90: 3187-3192.

O'Regan, B. and M. Gratzel, 1991. A low-cost, high-efficiency solar cell based on dye-sensitized colloidal TiO_2 films. Nature, 353: 737-740.

Park, S. and S. Yeo, 2008a. Recrystallization of caffeine using gas antisolvent process. J. Supercritical Fluids, 47: 85-92.

Park, S.J. and S.D. Yeo, 2008b. Recrystallization of phenylbutazone using supercritical fluid antisolvent process. Korean J. Chem. Engin., 25: 575-580.

Paulose, M., K. Shankar, O.K. Varghese, G.K. Mor, B. Hardin and C.A. Grimes, 2006. Backside illumination dye-sensitized solar cells based on titania nanotube array electrodes. Nanotechnology, 17: 1446-1448.r

Petit-Gas, T., O. Boutin, I. Raspo and E. Badens, 2009. Role of hydrodynamics in supercritical antisolvent processes. J. Supercritical Fluids, 51: 248-255.

Pollou, M., C.S. Malvi, D.W. Dixon-Hardy and R. Crook, 2009. Titanium wave-like surface microstructure for multiple reflection in solar cell substrates prepared by an all-solution process. Scripta Materialia, 62: 411-414.

Pu, Y., X. Tao, X. Zeng, Y. Le and J. Chen, 2010. Synthesis of Co-Cu-Zn doped Fe3O4 nanoparticles with tunable morphology and magnetic properties. J. Magnetism Magnetic Mater., 322: 1985-1990.

Reverchon, E. and R. Adami, 2006. Review of nanomaterials and supercritical fluids. J. Supercritical Fluids, 37: 1-22.

Reverchon, E., E. Torino, S. Dowy, A. Braeuer and A. Leipertz, 2009a. Interactions of phase equilibria, jet fluid dynamics and mass transfer during supercritical antisolvent micronization. Chem. Eng. J., 156: 446-458.

Reverchon, E., G. Della Porta and E. Torino, 2009b. Production of metal oxide nanoparticles by supercritical emulsion reaction. J. Supercritical Fluids, 53: 95-101.

Reverchon, E., I. De Macro and E. Torino, 2007. Nanoparticles production by supercritical antisolvent precipitation: A general interpretation. J. Supercrit. Fluids, 43: 126-138.

Reverchon, E., R. Adami, G. Caputo and I. De Marco, 2008. Review of Spherical microparticles production by supercritical antisolvent precipitation: Interpretation of results. J. Supercritical Fluids, 47: 70-84.

Shariati, A. and C.J. Peters, 2003. Recent developments in particle design using supercritical fluids. Curr Opin Solid State Mater. Sci., 7: 371-383.

Shi, J., J. Liang, S. Peng, W. Xu, J. Pei and J. Chen, 2009. Synthesis, characterization and electrochemical properties of a compact titanium dioxide layer. Solid State Sci., 11: 433-438.

Sierra-Pallares, J., E. Alonso, I. Montequi and M.J. Cocero, 2009. Particle diameter prediction in supercritical nanoparticle synthesis using three-dimensional CFD simulations. Validation for anatase titanium dioxide production. Chem. Eng. Sci., 64: 3051-3059.

Stengl, V., S. Bakardjieva and N. Murafa, 2009. Preparation and photocatalytic activity of rare earth doped TiO_2 nanoparticles. Mater. Chem. Phys., 114: 217-226.

Tang, Z.R., J.K. Edwards, J.K. Bartley, S.H. Taylor and A.F. Carley *et al.*, 2007. Nanocrystalline cerium oxide produced by supercritical antisolvent precipitation as a support for high-activity gold catalysts. J. Catalysis, 249: 208-219.

Tian, G., K. Pan, H. Fu, L. Jing and W. Zhou, 2009. Enhanced photocatalytic activity of S-doped TiO_2-ZrO_2 nanoparticles under visible-light irradiation. J. Hazardous Mater., 166: 939-944.

Tsai, T.Y. and S.Y. Lu, 2009. A novel way of improving wlight harvesting dye sensitized solar cells-electrodeposition of titania. Electrochemistry Commun., 11: 2180-2183.

Wang, Y., Y. Liu, H. Yang, H. Wang, H. Shen, M. Li and J. Yan, 2010. An investigation of DNA-like structured dye-sensitized solar cells. Curr. Applied Phys., 10: 119-123.

Xiaobo, C., 2009. Titanium dioxide nanomaterials and their energy applications. Chinese J. Catalysis, 30: 839-851.

Yu, K. and J. Chen, 2009. Enhancing solar cell efficiencies through 1-D nanostructures. Nanoscale Res. Lett., 4: 1-10.

Zhao, X., Y. Zu, Q. Li, M. Wang, B. Zu and X. Zhang, 2010. Preparation and characterization of camptothecin powder micronized by a supercritical antisolvent (SAS) process. J. Supercritical Fluids, 51: 412-419.